Molecular Crystals and Liquid Crystals
Publication details, including instructions for authors and subscription information:
http://www.tandfonline.com/loi/gmcl16

Low-Frequency Dielectric Relaxations in Nematics and Dual-Frequency Addressing of Field Effects

M. Schadt [a]
[a] F. Hoffmann-La Roche & Co., Central Research Units, 4002, Basel, Switzerland
Version of record first published: 13 Dec 2006.

To cite this article: M. Schadt (1982): Low-Frequency Dielectric Relaxations in Nematics and Dual-Frequency Addressing of Field Effects, Molecular Crystals and Liquid Crystals, 89:1-4, 77-92

To link to this article: http://dx.doi.org/10.1080/00268948208074471

Mol. Cryst. Liq. Cryst., 1982, Vol. 89, pp. 77–92
0026-8941/82/8904–0077$06.50/0

Printed in the United States of America

Low-Frequency Dielectric Relaxations in Nematics and Dual-Frequency Addressing of Field Effects

M. SCHADT

F. Hoffmann-La Roche & Co., Central Research Units, 4002 Basel, Switzerland

(*Received April 6, 1982*)

Novel low threshold nematic mixtures are presented exhibiting very low dielectric cross-over frequencies $f_c \simeq 1$ kHz at 20°C and unusually large, low- as well as high-frequency dielectric anisotropies $\Delta\epsilon_L > 4$ and $\Delta\epsilon_H < 4$ respectively. $\Delta\epsilon_L$ and $\Delta\epsilon_H$ are shown to be independently adjustable. The frequency and temperature dependence of the dielectric constants as well as the optical, elastic and viscous material constants are measured. Approximations are derived which quantitatively describe the influence of the LC material properties on the static electro-optical performance of dual-frequency addressed twisted nematic displays. It is shown that the number of multiplexable lines of dual-frequency addressed TN-LCDs comprising the new materials can be increased by more than a factor of 30 compared with conventional addressing. Moreover, very short turn-off times are reported.

I. INTRODUCTION

A number of studies have been reported on the dispersion of the parallel dielectric constant $\epsilon_\parallel$ in nematic liquid crystals.[1–4] Due to the liquid crystalline-specific intermolecular forces the dispersion region of $\epsilon_\parallel$ lies at exceptionally low frequencies compared with those of $\epsilon_\perp$ or $\epsilon_{isotropic}$.[2,4] The dispersion of $\epsilon_\parallel$ occurs in most nematics above 100 kHz at room temperature. However, a few materials have been reported exhibiting cross-over frequencies f_c in the 3–20 kHz range.[5–9] Since the change of sign of the dielectric anisotropy at f_c causes the nematic director to change its field-induced direction of alignment, dielectric dispersion

phenomena can in principle be used to influence the electro-optical properties of field-effects at relatively low frequencies.[6-13]

The question arose whether it would be possible to find nematic materials with very large static as well as high-frequency dielectric anisotropies which could be adjusted independently from each other. Moreover, to render the substances applicable the cross-over frequencies of such materials should remain very low, i.e. below ~2 kHz at room temperature. Other points of interest are the effects of low frequency dielectric relaxation phenomena and related liquid crystal material properties on the electro-optical performance of the twisted nematic effect[14] (TN-LCDs). The present study should also quantitatively give insight into the possibilities and limitations of dual-frequency addressing of TN-LCDs and its influence on their multiplexing performance.

2. DIELECTRIC PROPERTIES OF LOW CROSS-OVER FREQUENCY NEMATICS

2A. Basic concept

The strongly hindered rotation of nematic molecules around their short axes leads to the dispersion of the parallel dielectric constant $\epsilon_\parallel(\omega)$ with increasing angular frequency ω. At the cross-over frequency f_c the positive dielectric anisotropy $\Delta\epsilon$ can become zero; i.e. $\epsilon_\parallel(\omega_c = 2\pi f_c) = \epsilon_\perp$. Increasing ω further causes $\Delta\epsilon(\omega)$ to change sign. On the other hand the rotation around the long molecular axes is almost not hindered in nematics. As a consequence no dispersion of the perpendicular dielectric constant $\epsilon_\perp$ occurs up to microwave frequencies.[2] Since our interest focuses on low-frequency relaxation phenomena ($f < 100$ kHz), we shall in the following assume $\epsilon_\perp$ = constant.

Besides on temperature the low-frequency dispersion $\epsilon_\parallel(\omega)$ depends on molecular structural properties such as polarity, rigidity and length of the molecules and—in case of mixtures—on their composition. For a single relaxation process the frequency dependence of $\epsilon_\parallel(\omega)$ is given by[2]

$$\epsilon_\parallel(\omega) = \epsilon_\infty + \frac{(\epsilon_\parallel - \epsilon_\infty)}{1 + \omega^2\tau^2}, \quad \tau \propto \exp(E/kT); \tag{1}$$

where $\epsilon_\parallel = \epsilon_\parallel(\omega = 0)$ and $\epsilon_\infty = \epsilon_\parallel(\omega = \infty)$ are the static and the high-frequency parallel dielectric constants respectively. The relaxation time $\tau = 1/\omega_o$ in Eq. (1) is determined by the frequency where $\epsilon_\parallel(\omega_o) = (\epsilon_\parallel - \epsilon_\infty)/2$. According to the theory of Maier and Meier the dispersion step $(\epsilon_\parallel - \epsilon_\infty)$ in Eq. (1) increases for molecules with large longitudinal

permanent dipole moments $\hat{\mu}$:

$$(\epsilon_{\parallel} - \epsilon_{\infty}) = \frac{4\pi NhF^2}{3kT}\,\mu_{\parallel}^2(1 + 2S); \tag{2}$$

where N = Avogadro's number, h = cavity field factor, F = Onsager reaction field and S = nematic order parameter. Eq. (2) holds if $\hat{\mu}_{\parallel}$ coincides with the nematic director $\hat{n}$. From Eq. (2) follows that the dispersion step $(\epsilon_{\parallel} - \epsilon_{\infty})$ depends, like $\epsilon_{\parallel}$, essentially on $\hat{\mu}_{\parallel}$. $(\epsilon_{\parallel} - \epsilon_{\infty})$ and $\epsilon_{\parallel}$ are therefore interdependent parameters. $\epsilon_{\perp}$, on the other hand, does not depend on the parallel dielectric properties of the liquid crystal and is therefore independent from $\epsilon_{\parallel}$ and $(\epsilon_{\parallel} - \epsilon_{\infty})$. As a consequence it is in general not possible with a single liquid crystal component to achieve (a) a large dispersion step and (b) independently adjustable low- and high-frequency dielectric anisotropies $\Delta\epsilon_{\mathrm{L}} = \Delta\epsilon(\omega \ll \omega_c)$ and $\Delta\epsilon_{\mathrm{H}} = \Delta\epsilon(\omega \gg \omega_c)$ respectively. However, since $\Delta\epsilon$ of a binary mixture is related with $\Delta\epsilon^{\mathrm{A}}$ and $\Delta\epsilon^{\mathrm{B}}$ of its components A and B by[15]

$$\Delta\epsilon = m_{\mathrm{A}}\Delta\epsilon^{\mathrm{A}} + m_{\mathrm{B}}\Delta\epsilon^{\mathrm{B}}; \quad m_{\mathrm{A}} + m_{\mathrm{B}} = 1, \tag{3}$$

we are going to show that the above conditions as well as the requirement of a low cross-over frequency f_c can be realized in mixtures comprising at least two suitable components. m_{A} and m_{B} in Eq. (3) are the molar amounts of the components.

To render component A suitable we assume it to exhibit a large positive static dielectric anisotropy $\Delta\epsilon_{\mathrm{L}}^{\mathrm{A}} \gg 0$ and a low cross-over frequency f_c^{A} of $\epsilon_{\parallel}^{\mathrm{A}}(\omega)$. For component B we assume $\Delta\epsilon_{\mathrm{L}}^{\mathrm{B}} < 0$ and $f_c^{\mathrm{B}} \gg f_c^{\mathrm{A}}$. Then, from $\Delta\epsilon_{\mathrm{L}}^{\mathrm{A}} \gg 0$ and Eqs. (2) and (3) follows that the dispersion step $(\epsilon_{\parallel} - \epsilon_{\infty})$ of the mixture can be made large enough to cause its dielectric anisotropy $\Delta\epsilon(\omega)$ to change sign at f_c. The nematic director of the mixture will therefore align homeotropically at frequencies $f < f_c$ $(\hat{n} \parallel \hat{E})$, whereas for $f > f_c$ realignment into the homogeneous state occurs $(\hat{n} \perp \hat{E})$. Due to $f_c^{\mathrm{B}} \gg f_c^{\mathrm{A}}$ the low-frequency dispersion of $\epsilon_{\parallel}(\omega)$ and the height of the dispersion step of the mixture are essentially determined by the dispersion of molecules A only. However, molecules B may affect the onset of the dispersion via viscosity effects, thus causing f_c of the mixture to deviate from f_c^{A}. Since $\epsilon_{\perp}$ = constant holds up to microwave frequencies one obtains from Eqs. (1) and (3) for the frequency dependence of the dielectric anisotropy of a binary mixture comprising the above specified components A and B

$$\Delta\epsilon(\omega) = m_{\mathrm{A}}\left[\epsilon_{\infty}^{\mathrm{A}} + \frac{(\epsilon_{\parallel}^{\mathrm{A}} - \epsilon_{\infty}^{\mathrm{A}})}{1 + \omega^2\tau^2}\right] + m_{\mathrm{B}}\Delta\epsilon^{\mathrm{B}} - m_{\mathrm{A}}\epsilon_{\perp}^{\mathrm{A}}. \tag{4}$$

In the static limit Eqs. (3) and (4) are identical, i.e. $\Delta\epsilon(\omega \ll \omega_o) = \Delta\epsilon_L$. In the high frequency limit Eq. (4) becomes

$$\Delta\epsilon(\omega \gg \omega_c) = \Delta\epsilon_H = m_A(\epsilon_\infty^A - \epsilon_\perp^A) + m_B\Delta\epsilon^B. \quad (5)$$

Equations (3), (4) and (5) describe the static, the frequency-dependent and the high-frequency dielectric anisotropies of the mixture. They allow for a given pair of components with given dielectric properties to adjust the parameters $\Delta\epsilon_L$ and $\Delta\epsilon_H$ independently by choosing m_A and m_B appropriately. One can show that analogous equations hold for multicomponent mixtures if their components fulfill the above defined requirements.

2B. LC-materials and properties

To obtain large mesomorphic ranges as well as low crossover frequencies combined with rather low viscosities, three multicomponent mixtures $M1$, $M2$ and $M3$ were designed according to paragraph 2a using novel components† A and B. To experimentally determine the influence of the dielectric anisotropies $\Delta\epsilon_L$ and $\Delta\epsilon_H$ on the electro-optical performance of TN-LCDs (c.f. paragraph 3) the ratios $|\Delta\epsilon_H/\Delta\epsilon_L|$ of $M1$, $M2$ and $M3$ were chosen ~1, ~0.5 and ~2 respectively. The following four-ring esters used as components A exhibit very low crossover frequencies and large longitudinal permanent dipole moments:

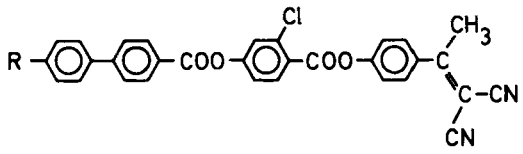

As strongly negative dielectric anisotropic compounds, pyridazines with the following structure were used:

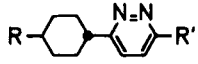

The static dielectric constants of component A measured at (T_c −10°C) are $\epsilon_\perp = 10.0$ and $\epsilon_\parallel = 26.3$ for R = C_6H_{13}; i.e. $\Delta\epsilon(A) = 16.3$. Extrapolation of dielectric measurements made in nematic binary mixtures

† The pyridazines were synthesized by Dr. G. Trickes, whereas the four-ring esters were synthesized by Dr. A. Villiger and Dr. M. Petrzilka of our laboratories. The synthesis and additional physical data of the new compounds will be published elsewhere.

gives $\epsilon_\perp = 15.5$ and $\epsilon_\parallel = 7.2$ at 10°C below the monotropic temperature T_c of the pyridazine with R = C_5H_{11} and R′ = C_3H_7; i.e. $\Delta\epsilon(B) = -8.3$. The melting and clearing temperatures (T_m, T_c) of compounds A and B are (118°C, 264°C) and (66°C, 14°C) respectively.

Figure 1 shows measurements of the temperature and frequency dependence $\epsilon_\parallel(\omega)$ and $\epsilon_\perp(\omega)$ of mixture $M1$. The results show that $M1$ exhibits a very low cross-over frequency $f_c = 1.4$ kHz at room temperature and large symmetric low- and high frequency dielectric anisotropies $\Delta\epsilon_L$ and $\Delta\epsilon_H$ respectively. The measurements confirm the assumption used in paragraph 2a that $\epsilon_\perp$ = constant in the frequency range studied. From Figure 1 it follows that virtually no dispersion of $\epsilon_\parallel(\omega)$ occurs for frequencies $f_L < 80$ Hz and temperatures as low as 10°C; i.e. $M1$ exhibits maximum positive dielectric anisotropy $\Delta\epsilon_L$. At the high frequency and temperature end $f_H \leqslant 50$ kHz is sufficient up to ~37°C to obtain maximum negative dielectric anisotropy $\Delta\epsilon_H$ (Figure 1). Thus, $M1$ allows full dual-frequency addressing between 10°C and 37°C with driving frequencies $f_L \leqslant 80$ Hz and $f_H \leqslant 50$ kHz respectively. At room temperature f_H can be reduced to 10 kHz (Figure 1).

Figure 2 shows dielectric relaxation measurements made at constant temperature $T = 22$°C using mixtures $M1$, $M2$ and $M3$. $M2$ and $M3$ exhibit—unlike $M1$—unsymmetrical anisotropies $\Delta\epsilon_L$ and $\Delta\epsilon_H$. Their cross-over frequencies are similar to $f_c(M1)$.

To characterize the temperature dependence of the dielectric disper-

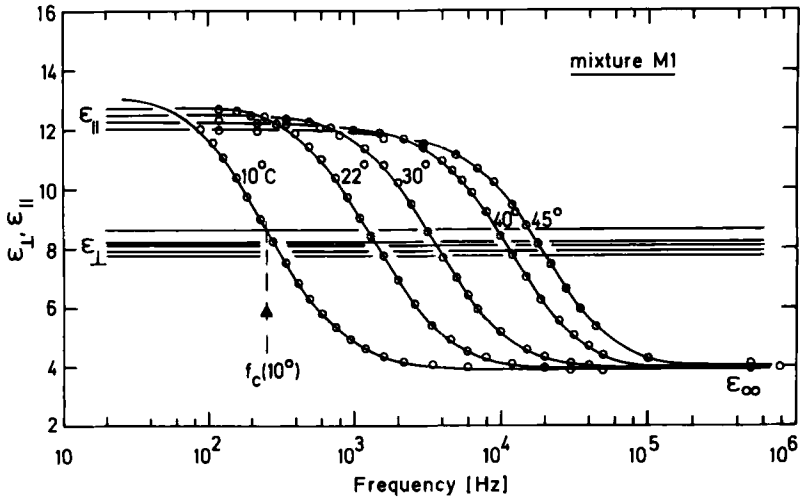

FIGURE 1 Measurements of the temperature and frequency dependences of $\epsilon_\parallel$ and $\epsilon_\perp$ of mixture $M1$.

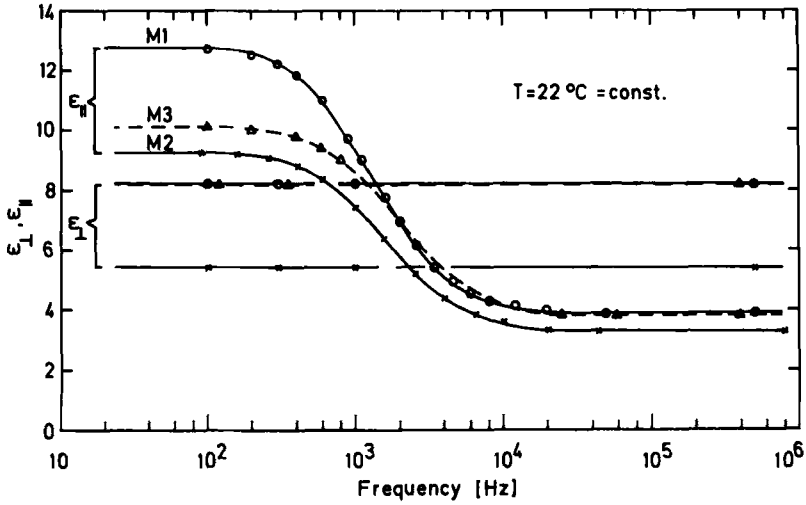

FIGURE 2 Frequency dependence $\epsilon_{\parallel}(f)$ of mixtures $M1$, $M2$ and $M3$ measured at $T = 22°C$ = constant. The measurements of $\epsilon_{\perp}$ show no frequency dependency.

sion, measurements of $f_c(1/T)$ of the three mixtures are plotted in Figure 3. The results show an exponential dependence with a rather large activation energy $E = 0.96$ eV for $M3$. The activation energies of $M1$ and $M2$ are comparable (Figure 3). f_c of all three mixtures does not exceed 20 kHz for temperatures $T \leqslant 40°C$ (Figure 3).

Table 1 summarizes the dielectric data of $M1$, $M2$ and $M3$ at 22°C. Besides, Table 1 shows measurements of the bulk viscosity η, the ordinary refractive index n_o measured at 550 nm, the optical anisotropy Δn, the splay (k_{11}), twist (k_{22}) and bend (k_{33}) elastic constants as well as the nematic-isotropic transition temperature T_c. It is interesting to note that the mixtures exhibit rather low k_{33}/k_{11} ratios that lead to steep transmission characteristics in conventionally, low-frequency driven TN-LCDs (c.f. paragraph 3). Moreover, Table 1 shows that the bulk viscosities are rather low considering the very low values for f_c and the high transition temperatures T_c. Thus, reasonably fast turn-on times of TN-LCDs operated at low driving frequencies can be expected. Table 1 shows that the material constants of $M1$, $M2$ and $M3$ are similar except for $\Delta\epsilon_L$ and $\Delta\epsilon_H$. Therefore, and because the mixtures can be blended among each other without leading to crystallization it is possible to adjust $|\Delta\epsilon_H/\Delta\epsilon_L|$ between ~0.5 and ~2 by blending.

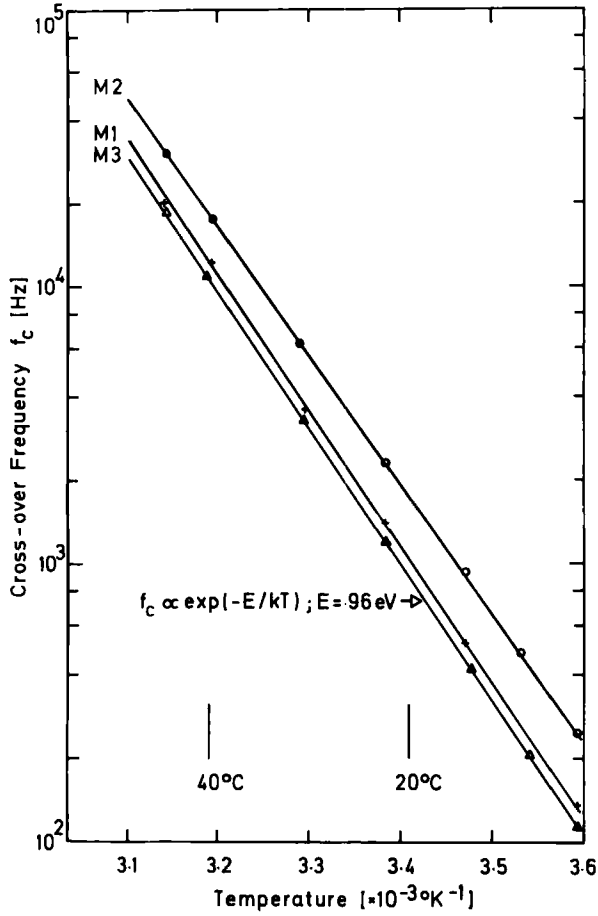

FIGURE 3 Measured temperature dependence of the cross-over frequency f_c of mixtures $M1$, $M2$ and $M3$.

3. DIELECTRIC RELAXATION AND STATIC ELECTRO-OPTICS OF FIELD-EFFECTS

3A. Theory

In the following it will be shown how dual-frequency addressing and liquid crystal material parameters affect and improve the transmission characteristics of TN-LCDs.

If a high frequency voltage $V(f \gg f_c) = V_H$ is superimposed on a low

TABLE I

Material properties of dual-frequency addressable mixtures M determined at 22°C. The melting temperatures of all mixtures are $T_m \simeq -5$°C. $\Delta\epsilon_L$ and $\epsilon_\parallel$ measured at $f = 80$ Hz, $\Delta\epsilon_H$ measured at $f = 10$ kHz [except for $\Delta\epsilon_H(f = \infty)$].

	$\epsilon_\parallel$	$\Delta\epsilon_L$	$\Delta\epsilon_H$	$\Delta\epsilon$(10 kHz)	f_c [kHz]	η [cP]	n_o	Δn	k_{11} [$x10^{-12}N$]	$\frac{k_{33}}{k_{11}}$	$\frac{k_{22}}{k_{11}}$	T_c [°C]
$M1$	12.75	4.42	−4.35	−4.10	1.40	85.8	1.493	0.105	11.8	1.06	0.54	78.3
$M2$	9.20	3.80	−2.12	−1.80	2.30	54.0	1.488	0.099	11.8	1.06	0.41	82.2
$M3$	10.25	2.15	−4.35	−3.80	1.20	65.7	1.489	0.099	13.1	1.00	0.50	74.5

frequency voltage $V(f \ll f_c) = V_L$ applied to a TN-LCD, the field-induced energy in the liquid crystal layer corresponding to a transmission of $X\%$ is given by

$$\Delta\epsilon_L V_X^2(V_H) - |\Delta\epsilon_H| V_H^2 = \Delta\epsilon_L V_X^2(V_H = 0). \tag{5}$$

Since LC-materials with low threshold voltages are desirable, $|\Delta\epsilon| > 0$ holds in practice. Therefore, and because the dielectric displacement $D = \epsilon_0\epsilon E =$ constant, the electric field E cannot be assumed to remain constant in the liquid crystal layer for voltages exceeding the threshold voltage V_c of the field-induced mechanical deformation of the helix. Strictly, Eq. (5) is therefore only correct for voltages $V \leqslant V_c$. However, to a first approximation and to obtain analytical expressions we shall assume in the following Eq. (5) to hold also for voltages exceeding V_c. Then, from the definition of the parameter $p = (V_{50} - V_{10})/V_{10}$ used to characterize the slope of the electro-optical transmission characteristics and from Eq. (5) follows:

$$V_{10}^2(V_H) \simeq V_{10}^2(V_H = 0) + \frac{|\Delta\epsilon_H|}{\Delta\epsilon_L} V_H^2$$

$$= \frac{V_{50}^2(V_H = 0)}{(1 + p_L)^2} + \frac{|\Delta\epsilon_H|}{\Delta\epsilon_L} V_H^2; \tag{6}$$

where V_{10} and V_{50} are the voltages required to obtain 10% and 50% transmission respectively; $p_L = p(V_H = 0)$. Equation (6) describes the shift of the transmission characteristics towards higher voltages which occurs when superimposing V_H on V_L.

To determine the influence of V_H and of the LC-material properties on the multiplexability of the cell, whose maximum number N_{max} of multiplexable lines can be described by[16]

$$N_{max} = \left[\frac{(1 + p)^2 + 1}{(1 + p)^2 - 1}\right]^2, \tag{7}$$

the dependence $p_H = p(V_H, \Delta\epsilon_L, \Delta\epsilon_H)$ has to be determined. Since an equation analogous to Eq. (6) holds for $V_{50}(V_H)$, one obtains from the definition of p and Eq. (6)

$$p_H \cong \left[\frac{(p_L + 1)^2 + \dfrac{|\Delta\epsilon_H|}{\Delta\epsilon_L}\left(\dfrac{V_H}{V_{10,L}}\right)^2}{1 + \dfrac{|\Delta\epsilon_H|}{\Delta\epsilon_L}\left(\dfrac{V_H}{V_{10,L}}\right)^2}\right]^{1/2} - 1, \tag{8}$$

where $V_{10,L} = V_{10}(V_H = 0)$. The parameter p_H in Eq. (8) characterizes

the slope of the transmission characteristics if a high-frequency voltage V_H is superimposed on V_L. Equation (8) shows that p_H decreases for increasing dielectric ratio $|\Delta\epsilon_H/\Delta\epsilon_L|$ and/or increasing voltage ratio $V_H/V_{10,L}$. The multiplexing improvement of dual-frequency addressing compared with single-frequency driving can be characterized by the following ratio which follows from Eq. (7):

$$\frac{N^H_{max}}{N^L_{max}} \cong \left[\frac{[(1+p_H)^2+1][(1+p_L)^2-1]}{[(1+p_H)^2-1][(1+p_L)^2+1]}\right]^2. \tag{9}$$

$N^L_{max} = N_{max}$ ($V_H = 0$) and $N^H_{max} = N_{max}$ (V_H) denote the respective maximum numbers of multiplexable lines in case of single and dual-frequency addressing. From Eqs. (8) and (9) and the low-frequency electro-optical parameters p_L and $V_{10,L}$ follows the dependence N^H_{max}/N^L_{max} versus a superimposed high-frequency voltage V_H.

The validity of Eqs. (6)–(9), whose low-frequency transmission parameters p_L, V_{10} and V_{50} implicitly contain the LC-material constants determining the electro-optical characteristics of the specific field-effect considered, is not restricted to TN-LCDs. The approximations are also applicable to other field effects as long as Eq. (5) holds. In case of zero bias tilt TN-LCDs the following recently derived analytical approximations[15] for p_L and V_{50} which hold for vertical light incidence can be inserted:

$$V_{50}(V_H = 0) \simeq V_c\left[2.044 - \frac{1.044}{2+\kappa}\right]\cdot \left[1 + 0.123(\gamma^{.6} - 1)\right]\cdot\left[1 + 0.132 ln\frac{\Delta nd}{2\lambda}\right] \tag{10}$$

$$p_L \cong 0.133 + 0.0266\kappa + 0.0443\left(ln\frac{\Delta nd}{2\lambda}\right)^2. \tag{11}$$

From the definition of p_L and the approximations in Eqs. (10) and (11) follows

$$V_{10}(V_H = 0) \cong V_{50}(V_H = 0)\cdot\left[0.88 - 0.024\kappa - 0.04\left(ln\frac{\Delta nd}{2\lambda}\right)^2\right]; \tag{12}$$

where $\kappa = (k_{33}/k_{11} - 1)$, $\gamma = \Delta\epsilon_L/\epsilon_\perp$, $\Delta n = (n_e - n_o)$, d = electrode spacing and λ = wavelength of transmitted light. For a 90° twisted helix the threshold voltage V_c of the field-induced mechanical deformation is given by

$$V_c = \pi\left[\frac{1}{\epsilon_0\Delta\epsilon_L}\left(k_{11} + \frac{k_{33} - 2k_{22}}{4}\right)\right]^{1/2}.$$

The approximations in Eqs. (6)–(12) describe the influence of the dielectric, the optical and the elastic LC-material constants as well as the influence of V_H on the electro-optical transmission characteristics of dual-frequency addressed TN-LCDs at vertical light incidence.

3B. Dual-frequency addressed TN-LCDs; experimental

The electro-optical measurements were performed in transmission at vertical light incidence using low bias tilt TN-LCDs ($\theta \simeq 2°$) with 10 μm electrode spacing and $\pi/4$ twist angle. The experiments were made at 22°C.

Figures 4 and 5 show transmission characteristics of TN-LCDs comprising mixtures $M2$ and $M3$ respectively. For each graph a different high-frequency voltage V_H characterized by the ratio $V_H/V_{10,L}$ = constant was used; where $V_{10,L} = V_{10}(V_H = 0)$ designates the conventional low frequency driving voltage required to obtain 10% transmission. The values of $V_{10,L}$ follow from the first graph on the left of each figure for which $V_H/V_{10,L} = 0$. The measurements in Figure 4 and Fig-

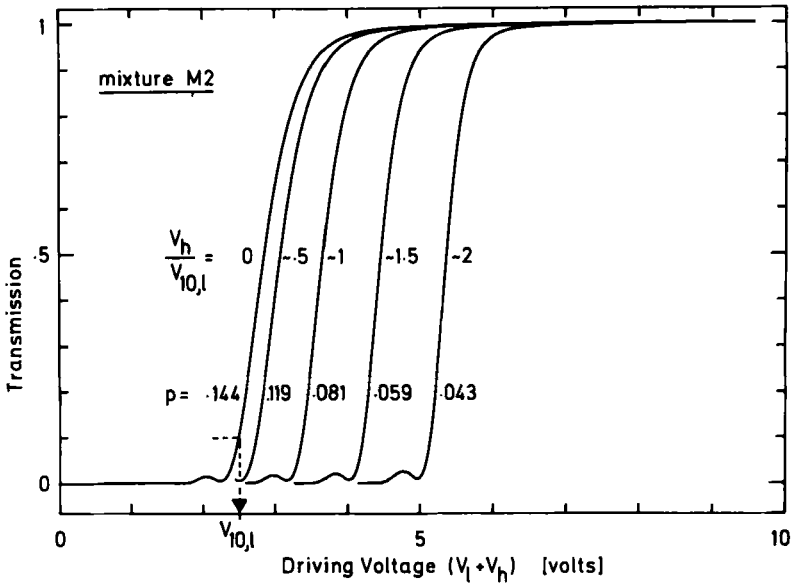

FIGURE 4 Transmission characteristics of TN-LCDs comprising mixture $M2$ recorded at 22°C at driving frequencies $f_L = 80$ Hz and $f_H = 10$ kHz respectively. The five graphs were recorded with V_H = constant superimposed on V_L. V_H for each graph follows from the voltage ratios $V_H/V_{10,L} = 0$, 0.572, 1.144, 1.716, 2.290 and from $V_{10,L} = 2.50$ volts. From the slopes of the transmission characteristics follow the indicated parameters p.

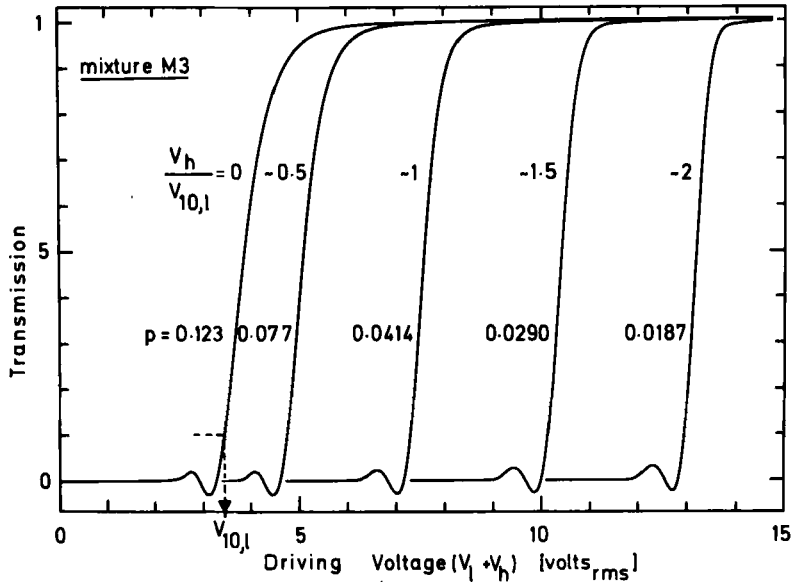

FIGURE 5 Transmission characteristics of TN-LCDs comprising mixture $M3$ measured at 22°C with driving frequencies $f_L = 80$ Hz and $f_H = 10$ kHz respectively. The respective constant high frequency driving voltages V_H applied during each recording follow from the voltage ratios $V_H/V_{10,L} = 0, 0.560, 1.123, 1.684, 2.245$ and from $V_{10,L} = 3.46$ volts.

ure 5 show that $M2$ with its low dielectric ratio $|\Delta\epsilon_H|/\Delta\epsilon_L$ compared with that of $M3$ (Table 1) leads to a considerably lower shift of the transmission characteristics with increasing voltage ratio $V_H/V_{10,L}$. Thus, while $M2$ whose threshold voltage $V_{10,L}$ is only 30% lower than that of $M3$ can still be operated at 6 volts for $V_H/V_{10,L} \cong 2$, $M3$ requires 14 volts (c.f. Figures 4 and 5). On the other hand the slopes of the transmission characteristics show a considerably greater increase for TN-LCDs comprising mixtures with large high frequency dielectric anisotropy, i.e. $|\Delta\epsilon_H|/\Delta\epsilon \gg 1$ (c.f. Figures 4 and 5 and Table 1). In the case of $M3$ this leads for $V_H/V_{10,L} \cong 2$ to a remarkable improvement of the maximum number of multiplexable lines compared with low-frequency addressing; i.e. $N^H_{max}/N^L_{max} = 39$ (Figure 5). These findings are qualitatively in agreement with Eqs. (6) and (8). Moreover, by inserting the respective material constants from Table 1 into Eqs. (10)–(12) it can be shown that the approximations (10)–(12) agree with the experimentally determined transmission values p_L, $V_{10,L}$ and $V_{50,L}$ within 5–10%.

To compare the measured dependence of the transmission characteristics on V_H and $|\Delta\epsilon_H|/\Delta\epsilon_L$ quantitatively with the approximation of

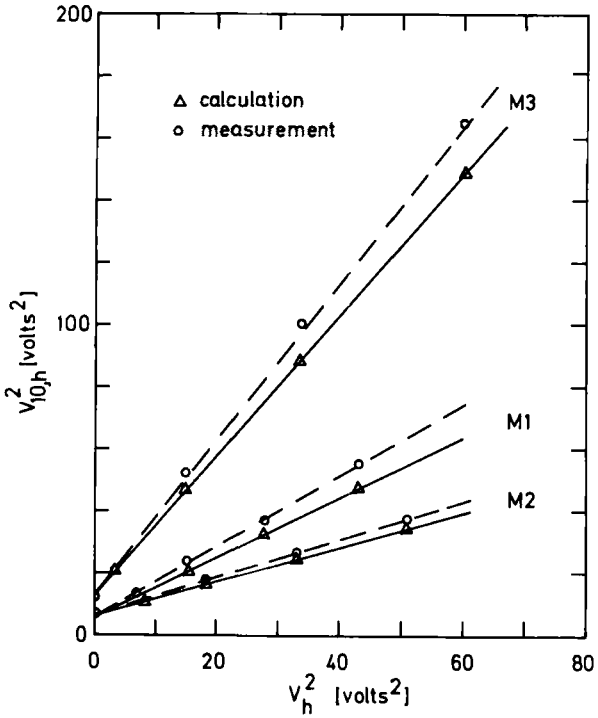

FIGURE 6 Measured and calculated dependence of the 10% transmission voltage $V_{10,H} = V_{10}(V_H)$ versus high frequency driving voltage V_H superimposed on V_L of TN-LCDs comprising the respective mixtures $M1$, $M2$ and $M3$. $T = 22°C$ = constant; $f_L = 80$ Hz, $f_H = 20$ kHz. $|\Delta\epsilon_H|/\Delta\epsilon_L$ of Table 1 and the measured voltages $V_{10,L}(M1) = 2.30$ volts, $V_{10,L}(M2) = 2.50$ volts and $V_{10,L}(M3) = 3.46$ volts were used for the calculation.

Eq. (6), plots of measured and calculated values of $V^2_{10,L}$ versus V^2_H are depicted in Figure 6. The straight lines obtained are in good agreement with the linear dependence $V^2_{10}(V_H) \propto V^2_H$ predicted by Eq. (6). Figure 6 shows that the values of $V_{10,H}$ calculated from Eq. (6) by using the measurements of $|\Delta\epsilon_H|/\Delta\epsilon_L$ (Table 1) and $V_{10}(V_H = 0)$ (c.f. text of Figure 6) deviate systematically by 10% from the measurements. However, considering the approximative character of Eq. (6) the agreement in Figure 6 is surprisingly good.

Figure 7 shows measured and from the approximation (9) calculated multiplexing ratios N^H_{max}/N^L_{max} plotted versus $V_H/V_{10,L}$ of TN-LCDs comprising mixtures $M1$, $M2$ and $M3$. The parameters p_H in Eq. (9) were determined from Eq. (8) using $|\Delta\epsilon(10\text{kHz})|/\Delta\epsilon_L$ of Table 1 and measurements of p_L. Comparing measured and calculated graphs in

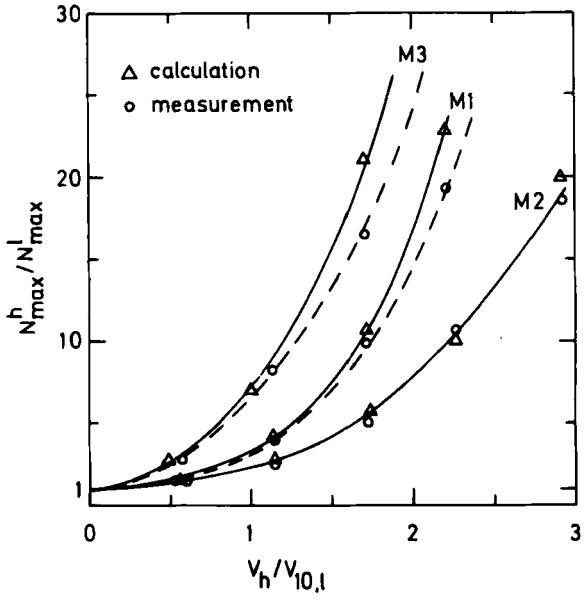

FIGURE 7 At 22°C measured and calculated multiplexing ratios N^H_{max}/N^L_{max} versus voltage ratio $V_H/V_{10}(V_H)$ of TN-LCDs comprising mixtures $M1$, $M2$ and $M3$ respectively; $f_L = 80$ Hz, $f_H = 10$ kHz.

Figure 7 shows that approximation (9) verifies the improved multiplexing performance of dual-frequency addressing compared with conventional addressing rather well for LC-materials with $|\Delta\epsilon_H|/\Delta\epsilon_L \lesssim 1$ and high-frequency voltages $V_H \lesssim 2V_{10,L}$. For materials with $|\Delta\epsilon_H|/\Delta\epsilon_L \gg 1$ and $V_H \gtrsim 1.5$ increasingly strong deviations occur between measurement and calculation (c.f. graphs for $M3$ in Figure 7).

Due to the change of sign of the dielectric anisotropy which occurs when changing the driving frequency of the display voltage from $f_L \rightarrow f_H$, very fast turn-off times can be obtained with dual-frequency addressable LC-materials. The measurements in Figure 8 show an example for the response improvement upon actively switching a TN-LCD. The active turn-off time t^{L-H}_{off} turns out to be 17-times faster than the passive turn-off time t^L_{off} (Figure 8). Since both signals $S1$ and $S2$ induce the same field-induced angular momentum when switching the display on at $t = 0$ (Figure 8), the turn-on time t^L_{on} induced by the gated signal $S1$ is identical to that corresponding to the frequency change $f_H \rightarrow f_L$ of $S2$.

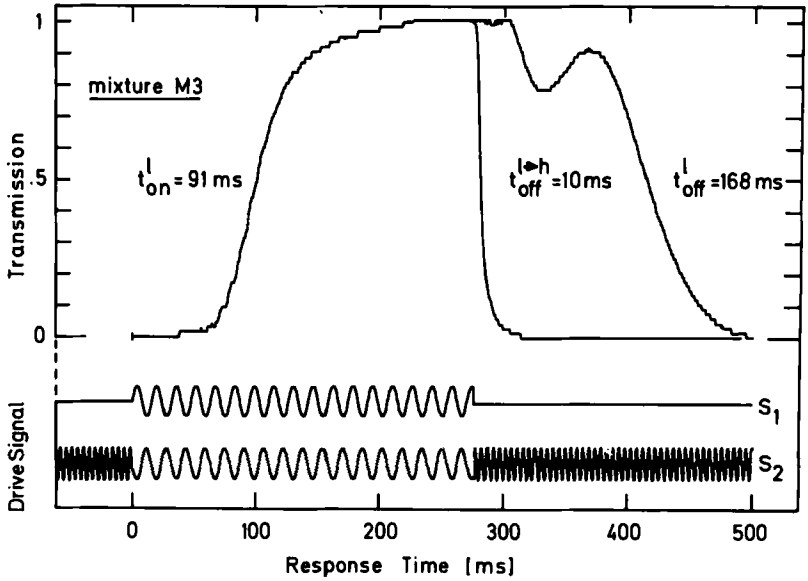

FIGURE 8 Electro-optical response measurements of a TN-LCD comprising mixture *M3*; electrode spacing $d = 10\ \mu m$. The turn-on time t^{L}_{on} (0–50%) and the turn-off time t^{L}_{off} (100–10%) correspond to the conventional low frequency gated driving signal S_1 applied at time $t = 0$ to the display. The 80 Hz rms voltage of S_1 is $3 \cdot V_{10,L} = 10.4$ volts. The turn-off time $t^{L\to H}_{off}$ (100–10%) correspond to the driving signal *S2* whose rms voltage of 10.4 volts remains constant but whose driving frequency is switched from $f_L = 80$ Hz to $f_H = 10$ kHz and vice versa at the times indicated by *S2* at the bottom of the Figure.

4. CONCLUSIONS

It could be shown that dual-frequency addressable nematic liquid crystals with exceptionally low cross-over frequencies, $f_c \sim 1$ kHz, rather low viscosity and independently adjustable low- and high-frequency dielectric anisotropies $\Delta\epsilon_L = (\epsilon_{\parallel} - \epsilon_{\perp})$ and $\Delta\epsilon_H = (\epsilon_{\infty} - \epsilon_{\perp})$ can be made by blending suitable strongly positive dielectric anisotropic nematics with suitable negative dielectric materials. The frequency- and composition dependence of the dielectric properties are shown. To study the influence of $\Delta\epsilon_L$ and $\Delta\epsilon_H$ on the electro-optical performance of displays, three nematic mixtures were investigated with ratios $|\Delta\epsilon_H|/\Delta\epsilon_L$ ranging from 0.5–2. Their dielectric, elastic, optical and viscous material properties were quantitatively related with their electro-optical performance in twisted nematic displays.

Measurements of the electro-optical transmission characteristics of

TN-LCDs comprising dielectrically strongly different nematics were compared with analytical approximations derived to describe the influence of dual-frequency addressing and LC-material properties on the multiplexability and operating voltage of TN-LCDs. It could be shown that rather low operating voltages, very fast turn-off times and—compared with conventionally driven displays—remarkably increased multiplexing ratios $N^{H}_{max}/N^{L}_{max} > 30$ can be achieved. The results indicate that high information density displays with multiplexing ratios up to ~250:1 that can be operated in the temperature range ~10°C to ~40°C are feasible.

Acknowledgment

I am very much indebted to M. Petrzilka, A. Villiger and G. Trickes, who synthesized the four-ring esters and the pyridazines. I also gratefully acknowledge the skilled assistance of B. Blöchliger in the performance of the experiments and wish to thank P. Gerber for helpful discussions.

References

1. W. Maier and G. Meier, *Z. Naturforsch.*, **16a**, 262 (1961).
2. M. Schadt, *J. Chem. Phys.*, **56**, 1494 (1972) and *J. Chem. Phys.*, **67**, 210 (1977).
3. D. Diguet, F. Rondelez and G. Durand, *C. R. Acad. Sci. Ser.*, **B271**, 954 (1970).
4. M. Schadt and C. von Planta, *J. Chem. Phys.*, **63**, 4379 (1975).
5. W. H. de Jeu, C. J. Gerritsma, P. Van Zanten and W. J. A. Goossens, *Phys. Lett.*, **39A**, 355 (1972).
6. G. Baur, A. Stieb and G. Meier in *Ordered Fluids and Liquid Crystals*, **2**, 645 by Porter and Johnson (Plenum, 1974).
7. H. K. Bücher, R. T. Klingbiel and J. P. Van Meter, *Appl. Phys. Lett.*, **25**, 186 (1974).
8. H. Nakamura, German Offenlegungsschrift Nr. 2856134 (1979).
9. P. R. Gerber, *Z. Nat. Forsch.*, to be published.
10. T. S. Chang and E. E. Loebner, *Appl. Phys. Lett.*, **25**, 1 (1974).
11. D. Pötsch and W. Haase, *Phys. Lett.*, **57A**, 343 (1976).
12. C. Z. Van Doorn and J. J. de Klerk, *J. Appl. Phys.*, **50**, 1066 (1979).
13. C. S. Bak, K. Ko and M. M. Labes, *J. Appl. Phys.*, **46**, 1 (1975).
14. M. Schadt and W. Helfrich, *Appl. Phys. Lett.*, **18**, 127 (1971).
15. M. Schadt and P. R. Gerber, *Z. Nat. Forsch.*, **37A**, 165 (1982).
16. P. M. Alt and P. Pleshko, *IEEE Trans. Electron Dev.*, **ED-21**, 146 (1974).